AWARD NUMBER: W81XWH-18-1-0690

TITLE: Therapeutic Targeting of Neuroendocrine Prostate Cancer

PRINCIPAL INVESTIGATOR: Eva Corey

CONTRACTING ORGANIZATION: University of Washington

REPORT DATE: SEPTEMBER 2020

TYPE OF REPORT: Annual

PREPARED FOR: U.S. Army Medical Research and Development Command
Fort Detrick, Maryland 21702-5012

DISTRIBUTION STATEMENT: Approved for Public Release;
Distribution Unlimited

REPORT DOCUMENTATION PAGE

Form Approved
OMB No. 0704-0188

1. REPORT DATE	2. REPORT TYPE	3. DATES COVERED
SEPTEMBER 2020	ANNUAL	9/1/2019-8/31/2020

4. TITLE AND SUBTITLE

Therapeutic Targeting of Neuroendocrine Prostate Cancer

5a. CONTRACT NUMBER
W81XWH-18-1-0690

5b. GRANT NUMBER
PC170350P2

5c. PROGRAM ELEMENT NUMBER

6. AUTHOR(S)
Eva Corey

E-Mail: ecorey@uw.edu

5d. PROJECT NUMBER

5e. TASK NUMBER

5f. WORK UNIT NUMBER

7. PERFORMING ORGANIZATION NAME(S) AND ADDRESS(ES)

University of Washington
4333 Brooklyn Ave
Seattle WA 98195-9472

8. PERFORMING ORGANIZATION REPORT NUMBER

9. SPONSORING / MONITORING AGENCY NAME(S) AND ADDRESS(ES)

U.S. Army Medical Research and Development Command
Fort Detrick, Maryland 21702-5012

10. SPONSOR/MONITOR'S ACRONYM(S)

11. SPONSOR/MONITOR'S REPORT NUMBER(S)

12. DISTRIBUTION / AVAILABILITY STATEMENT

Approved for Public Release; Distribution Unlimited

13. SUPPLEMENTARY NOTES

14. ABSTRACT

Neuronedocrine prostate cancer is an advanced form of this disease with very limited option of effective treatment. It has been shown that BRN2 is highly expressed in NEPC, and preliminary in vitro data show that inhibition of BRN2 decreases tumor cells growth. We will perform preclinical evaluation of efficacy of a novel BRN2 inhibitor alone, in combination with carboplatin (a standard therapy for neuroendocrine prostate cancer) to determine whether this treatment inhibits progression of NEPC and provides survival benefits.

15. SUBJECT TERMS

NONE LISTED

16. SECURITY CLASSIFICATION OF:			17. LIMITATION OF ABSTRACT	18. NUMBER OF PAGES	19a. NAME OF RESPONSIBLE PERSON
a. REPORT	b. ABSTRACT	c. THIS PAGE			USAMRMC
Unclassified	Unclassified	Unclassified	Unclassified	16	19b. TELEPHONE NUMBER *(include area code)*

TABLE OF CONTENTS

INTRODUCTION

Prostate Cancer (PCa) is the most common male cancer and the 2nd leading cause of cancer deaths in North American men. While advanced PCa is initially controlled with hormonal therapies targeting the androgen receptor (AR) pathway, recurrence occurs due to emergence of lethal castration-resistant PCa (CRPC). Despite the potency of AR pathway inhibitors (ARPI) such us Enzalutamide (ENZ) that prolong survival, resistance ultimately emerges. Autopsy series suggest that up to 25% of CRPC patients resistant to ARPIs shed their dependence on the AR and exhibit a continuum of features associated with the neuroendocrine (NE) lineage (1). The diagnosis of Neuroendocrine Prostate Cancer (NEPC) is accompanied by a dismal overall survival measured in months, with decades old cytotoxic chemotherapy as standard treatment (2-4). Targeted treatments for this deadly disease are desperately needed. We were the first group to report that BRN2, a neuronal transcription factor, is sufficient and required to drive the evolution of an AR-driven adenocarcinoma into an aggressive and lethal AR-indifferent NEPC tumor (5). We have since developed a highly specific and potent small molecule BRN2 inhibitor (BRN2i). This project is centered on testing a new paradigm that epigenetic reprogramming, driven by BRN2, represents a molecular "conduit" to aggressive NEPC. In particular, how does BRN2 alter the architecture of the epigenome? Does BRN2 activate/regulate an intrinsic neurogenesis program? Can BRN2i prevent and/or treat NEPC?

To answer these questions, proposed a highly collaborative effort using innovative prostate cancer models coupled with state-of-the-art technologies, a series of ENZ-resistant (ENZR) including t-NEPC (5) and a large cohort of prostate cancer patient-derived xenografts. These established and novel PDX models serve as patient "avatars" that will ensure our research is relevant and rapidly translatable for treatment of aggressive prostate cancer, with immediate applications including; 1) deciphering the mechanisms underlying cellular plasticity leading to treatment resistance in PCa after hormone therapy; 2) exploring temporal changes in genetics/epigenetics during treatment-induced progression from adenocarcinoma to NEPC, and 3) testing therapeutic schemes, for example, when to best deploy BRN2i and whether they should be used as a monotherapy or in combination.

These studies will provide insight into how the epigenome is reprogrammed during the transition from an adenocarcinoma to NEPC in response to ARPIs by assessing fluxes in chromatin architecture and identifying the importance of BRN2 in mediating these processes. Our research posits that blocking that ability of cells to acquire a plastic phenotype via BRN2 inhibitor may delay/inhibit lineage transformation and extend the durability of clinically beneficial ARPIs and/or treat NEPC.

BODY

Key research Accomplishments

As indicated in the statement of work, year 2 (months 12-24) of this PCRP-Idea Award, consists of experiments outlined in all 3 Aims. While greatly diminished due to research restrictions imposed for the COVID 19 pandemic, we were able to conduct key experiments and optimize some assays for future use.

- Conducted ATAC-seq on tNEPC (42D) and de novo NEPC cells to gain access to both accessible DNA and nucleosome positioning data.
- Conducted ChIP-seq for histone modifications on tNEPC cells and mapped BRN2 binding relative to accessible and transcriptionally active or inactive regions. We then combined this information with phenotype data upon BRN2 knockout and inhibition to understand how the BRN2 cistrome relates to NEPC.
- Identified and validated BRN2 binding to SWI/SNF complex.
- Optimized a custom ELISA assay for secreted protein IGFBP5 and tested against BRN2 knockdown/inhibition as well as AR inhibition.
- *In vivo* studies in PDX models with lead BRN2 inhibitor are ongoing. In addition to our initial studies reported in Y1, we also compared efficacy of BRN2 inhibitor against standard of care chemotherapy Carboplatin in de novo NEPC model NCI-H660.

REPORTABLE OUTCOMES

Aim 1

In an effort to understand the molecular mechanisms by which BRN2 promotes such a strong reprogramming towards a neuronal phenotype, we conducted ChIP-seq for BRN2 in our tNEPC cell line (42D) and de novo SCNC cell line NCI-H660. Overall, the binding pattern between $42D^{ENZR}$ and NCI-H660 was pretty similar, with H660 cells having more promoter binding **(Fig 1A)**. Interestingly, pathways enriched in BRN2 bound loci (cistrome) mapped to genes belonging to Neurogenesis, Neuron Fate Differentiation and Cell Cycle progression pathways **(Figure 1B-C)**. Next, we overlaid BRN2 binding with ATAC-seq data which identifies open regions of chromatin and we discovered that a majority of BRN2 binding occurs in closed regions of chromatin **(Figure 1D)**. This ability to bind to closed regions of chromatin and regulate gene expression is held by a class of transcription factors known as pioneer factors (6). Our finding regarding pioneering capabilities of BRN2 is consistent with recent biophysical experiments that reported BRN2 preferentially binds to nucleosomal DNA (closed chromatin) as opposed to open DNA (7).

In order to better characterize the observed BRN2 cistrome, we focused on $42D^{tNEPC}$ cells conducted ChIP-seq for histone marks for transcriptionally active marks (H3K4me3 and H3K27ac) along with H3K27me3 for transcriptional inactivity and mapping them to our ATAC-seq data **(Fig 2A)**. Loci possessing either active histone mark (K4me3 vs K27Ac) were relatively equal in signal intensity **(Fig 2B)**. However, a locus with double positive for K4me3 and K27Ac modification was significantly more open/active; bringing the total to 13389 peaks in open chromatin with both active histone marks **(Fig 2C)**. We also observed loci positive for H3K4me3 (active) and H3K27me3 (inactive) existing in partially open chromatin, a typical feature of bivalent loci (4182 peaks) **(Fig 5D)** which are either poised for activity/inactivity or heterogeneously active/inactive within the cell population (8). These bivalent regions also possess an overall signal intensity comparable to regions with one active chromatin mark (K4me3 or K27Ac). Most other loci unique to either of the three histone modifications were present in closed regions of chromatin.

Next, we overlaid these histone marks with the BRN2 cistrome and immediately observed a few striking facts; BRN2 binding exists at 80% of all K4me3 loci, 56% of K27Ac loci and a staggering 81% (10864/13389) of double positive loci **(Fig 3A, F)**. These data implicate BRN2 as a vital regulator of the baseline transcriptionally active epigenetic state of $42D^{tNEPC}$ cells. BRN2 also overlaps with 23% of all with H3K27me3 binding sites, however, out of these 7155 peaks, 3424 (48%) are bivalent as they are co-occupied by K4me3. Again, BRN2 binds at 3424/4182 (81%) of all bivalent sites in the $42D^{tNEPC}$ cistrome **(Fig 3A, F)**. Taking this analysis one step further, we incorporated ATAC-seq data into the BRN2/histone ChIP-seq and subset BRN2 binding into "Closed", "Hyper" and "Bivalent" regions and de-convoluted some of the phenotypes such as cell proliferation and neurogenesis that appear to be governed by BRN2 **(Fig 3B-D)**.

BRN2 binding sites co-occupied by both H3K4me3 and H3K27Ac exist in hyper-accessible regions of chromatin and primarily in the promoters (54%) of genes belonging to cell cycle and cell proliferation pathways **(Fig 3D-E)**. Similarly, BRN2 binding sites overlapping with H3K4me3 (active) and H3K27me3 (inactive) partially exist in open chromatin, a typical feature of bivalency. Moreover, the binding of BRN2 at these cites once again occurs primarily in the promoter (44%)

however these genes belong specifically to neurogenesis and bivalency pathways in brain cells **(Fig 3D-E)**. Lastly, BRN2 binding in closed regions of chromatin unaccompanied by the above-mentioned histone marks are largely intergenic/intronic and enriched for genes typically bound by Polycomb Repressor Complex 2 (PRC2) in embryonic stem cells **(Fig 3D-E)**. Importantly, these exact pathways are significantly downregulated in cells upon CRISPR/Cas9 mediated knockout of BRN2 or BRN2 inhibition by small molecule, explicitly linking BRN2 binding to the functional regulation of genes involved in NE differentiation and cell cycle progression **(Fig 4A-C)**.

Future direction/experiments: These experiments subset the observed BRN2 cistrome and explain some of the phenotypes observed upon BRN2 inhibition. In the upcoming year, I plan to expand this analysis by exploring the BRN2 interactome through Rapid Immunoprecipitation and Mass Spectrometry (RIME) and figure out the interactions that guide/define BRN2 binding in the cistrome. These experiments will include both $42D^{tNEPC}$ and NCI-H660 model to delineate any possible similarities and differences in BRN2 function between treatment induced and de novo NEPC.

Aim 2

As reported in Y1, we were able to test our BRN2 inhibitor *in vivo* with $42D^{tNEPC}$ and NCI-H660 xenograft models. Our current lead BRN2 inhibitor significantly reduces tumor volume in both xenograft models and downregulates expression of Ki67, BRN2 and downstream markers. Using the H660 model, we also compared the efficacy of BRN2i to standard of care platinum-based chemotherapy. The 50mg/kg dose of BRN2i demonstrated comparable anti-tumor activity to 20mg/kg (thrice weekly) dose of carboplatin without the accompanying toxicity leading to body weight loss **(Figure 4A-B)**.

In Y2 we also performed two studies using NEPC PDX model, LuCaP 93 and LuCaP 145.2 to evaluate the efficacy of BRN2i. Unfortunately, in contrast to studies with cell line xenografts, in both of the LuCaP PDX studies, we observed due to an acute toxicity event and we had to lower to dose from 50mg/kg to 30mg/kg. Consequently, treatment with the BRN2i did not show any significant anti-tumor activity within the animals that survived. We hypothesize that low dose of the inhibitor used was the reason for these results and we are proceeding to evaluate whether the BRN2 signalling was inhibited in the treated tumors using immunohistochemistry.

To address this issue, we ran a small toxicity study using CB17 SCID mice (used in the LuCaP studies) with a new batch of the BRN2i, with increasing dose from 30 to 50 to 75 up to 100mg/kg. In this experiment, all the doses were well tolerated. Our working hypothesis is that the previously observed toxicity in the studies performed at UW might be related to a specific batch of the inhibitor and we are in the process of analyzing the compounds from both batches. Currently, we are setting up two new studies using NEPC PDX LuCaP 49 and LuCaP 173.1. using the BRN2i that did not show toxicity and plan to treat with 50 mg/kg.

Aim 3

For this aim, our goal is to validate IGFBP5 as a pharmacodynamics marker for BRN2 activity as well as explore its potential as a marker for NE-transdifferentation. Our preliminary data demonstrated that IGFPB5 was upregulated in NEPC patient samples, PDX models and in our tNEPC $42D^{ENZR}$ cell line model **(Fig. 5A-C)**. Importantly, we show that levels of IGFBP5 in media of $42D^{ENZR}$ cells decreases upon treatment with BRN2 inhibitor or knockdown by siRNA **(Fig. 5D)**. Our goal is to measure levels of IGFBP5 in a non-invasive manner and therefore these

results required validation by ELISA. We purchased over five different commercially available ELISA kits including some that were used in previous publications and some that were not. Unfortunately, all the kits failed to detect BP5 efficiently; while they were able to detect positive control peptide, all the kits failed negative controls and demonstrated strong non-specific binding. In an attempt to optimize the existing ELISA kits, we used different combination of antibodies to create a custom sandwich ELISA protocol using antibodies both from the kits and from other vendors and different sample preparations including protein denaturation. Our preliminary data showed that we successfully optimized the ELISA using denatured protein (b-mercaptoethanol and boiling) as well as using monoclonal antibody targeting the N-terminal and a polyclonal antibody. Our preliminary data showed significantly increased levels of IGFBP5 in media from $42D^{ENZR}$ cells in comparison to $16D^{CRPC}$ cells, consistent their mRNA expression levels. Lastly, as an important validation for measurement if IGFBP5 as a BRN2 response gene, we can so that upon inhibition of BRN2 in $42D^{ENZR}$ using our small molecule inhibitor induced a decrease of secreted IGFBP5 **(Fig. 5E)**. With this working ELISA protocol, we will move forward with testing samples from our xenograft and PDX studies to validate measurement of serum-IGFBP5 as a pharmacodynamic for BRN2 inhibition.

To test whether measuring levels of IGFBP5 is a viable strategy for capturing NE-transdifferentiation we measured IGFBP5 levels upon AR inhibition. The literature around changes in IGFBP5 expression in this context is contradictory. In 1999, Gregory et al. demonstrated that intracellular protein levels of IGFBP5 decrease upon castration (9); while in the year 2000 Miyaki et al. showed that IGFBP5 mRNA levels increase upon castration (10). Similarly, samples from Neo Adjuvant hormone-therapy patients also showed increased IGFBP5 mRNA expression **(Fig. 6A)** (11). Our optimized ELISA assay allowed us to confirm that both published scenarios are indeed true. IGFBP5 mRNA increases after ENZ treatment in $16D^{CRPC}$ cells, but its protein levels in cell lysate decreased **(Fig. 6B)**. Importantly however, the amount of IGFBP5 in the media increases significantly **(Fig. 6C)**. Altogether with previously published data, we can conclude that AR inhibition indeed induces IGFBP5 mRNA expression but the intracellular levels if IGFBP5 decrease because it is secreted into the media at an increased rate.

CONCLUSION

BRN2 functions as a pioneer factor in NEPC: In t-NEPC $42D^{ENZR}$ model, BRN2 binds to both open and closed regions of chromatin. Moreover, the BRN2 cistrome is primarily linked to the transcriptionally active genes as 81% of H3K4me3 and H3K27Ac (Hyper-active) and 81% of H3K4me3 and H3K27me3 (Bivalent) genomic loci are co-occupied by BRN2. Importantly, these exact genes/pathways are simultaneously downregulated by BRN2 knockout or inhibition via small molecule.

IGFBP5 as a marker for BRN2 activity and NE-differentiation: In the absence of a functioning commercially available ELISA kit, we have developed a custom antibody ELISA sandwich that allows us to accurately measure secreted levels of IGFBP5. With this assay, we have demonstrated for the first-time enhanced secretion IGFBP5 upon AR inhibition and importantly in tNEPC model, inhibition of BRN2 reduces IGFBP5 mRNA and subsequent protein production and secretion as measurable by qPCR, WB and ELISA.

PUBLICATIONS

Title – "Selective inhibition of transcription factor BRN2 as a treatment strategy for Small Cell Prostate Cancer"

Thaper D, Munuganti R, Aguda A, Ku S, Kumar S, Kim S, Vahid S, Sivak O, Puca L, Bishop JL, Morrissey C, Corey E, Beltran H and Zoubeidi A

1. Poster presentation at AACR Virtual Annual Meeting II (2020)
2. Invited Talk at AACR Advances in Prostate Cancer Research (2020), Denver, CO, USA *cancelled due to COVID19*
3. Poster presentation at Prostate Cancer Foundation Annual Retreat (2019), Carlsbad, CA, USA (2019)
4. Poster presentation at the FEBS Workshop: Nuclear Receptors, Spetses Island, Greece (2019)

INVENTIONS, PATENTS AND LICENSES

None

References

1. Bluemn EG, Coleman IM, Lucas JM, Coleman RT, Hernandez-Lopez S, Tharakan R, et al. Androgen Receptor Pathway-Independent Prostate Cancer Is Sustained through FGF Signaling. Cancer Cell. 2017;32(4):474-89 e6.
2. Eric Jay Small JH, Jack Youngren, Artem Sokolov, Rahul Raj Aggarwal, George Thomas, Lawrence D. True, Li Zhang, Adam Foye, Joshi J. Alumkal, Charles J. Ryan, Matthew Rettig, Christopher P. Evans, Martin Edwin Gleave, Robert Baertsch, Josh Stuart, Robert Evan Reiter, Primo Lara, Kim N. Chi, Tomasz M. Beer. Characterization of neuroendocrine prostate cancer (NEPC) in patients with metastatic castration resistant prostate cancer (mCRPC) resistant to abiraterone (Abi) or enzalutamide (Enz): Preliminary results from the SU2C/PCF/AACR West Coast Prostate Cancer Dream Team (WCDT). J Clin Oncol. 2015;33.
3. Aparicio A, Logothetis CJ, Maity SN. Understanding the lethal variant of prostate cancer: power of examining extremes. Cancer discovery. 2011;1(6):466-8.
4. Robinson D, Van Allen EM, Wu YM, Schultz N, Lonigro RJ, Mosquera JM, et al. Integrative clinical genomics of advanced prostate cancer. Cell. 2015;161(5):1215-28.
5. Bishop JL, Thaper D, Vahid S, Davies A, Ketola K, Kuruma H, et al. The Master Neural Transcription Factor BRN2 Is an Androgen Receptor-Suppressed Driver of Neuroendocrine Differentiation in Prostate Cancer. Cancer discovery. 2017;7(1):54-71.
6. Schlesinger S, Meshorer E. Open Chromatin, Epigenetic Plasticity, and Nuclear Organization in Pluripotency. Dev Cell. 2019;48(2):135-50.
7. Fernandez Garcia M, Moore CD, Schulz KN, Alberto O, Donague G, Harrison MM, et al. Structural Features of Transcription Factors Associating with Nucleosome Binding. Mol Cell. 2019;75(5):921-32 e6.
8. Bernstein BE, Mikkelsen TS, Xie X, Kamal M, Huebert DJ, Cuff J, et al. A bivalent chromatin structure marks key developmental genes in embryonic stem cells. Cell. 2006;125(2):315-26.
9. Gregory CW, Kim D, Ye P, D'Ercole AJ, Pretlow TG, Mohler JL, et al. Androgen receptor up-regulates insulin-like growth factor binding protein-5 (IGFBP-5) expression in a human prostate cancer xenograft. Endocrinology. 1999;140(5):2372-81.
10. Miyake H, Pollak M, Gleave ME. Castration-induced up-regulation of insulin-like growth factor binding protein-5 potentiates insulin-like growth factor-I activity and accelerates progression to androgen independence in prostate cancer models. Cancer Res. 2000;60(11):3058-64.
11. Beltran H, Wyatt AW, Chedgy EC, Donoghue A, Annala M, Warner EW, et al. Impact of Therapy on Genomics and Transcriptomics in High-Risk Prostate Cancer Treated with Neoadjuvant Docetaxel and Androgen Deprivation Therapy. Clin Cancer Res. 2017;23(22):6802-11.

APPENDIX

Figure 1 – Chromosome Accessibility in PCa cell lines

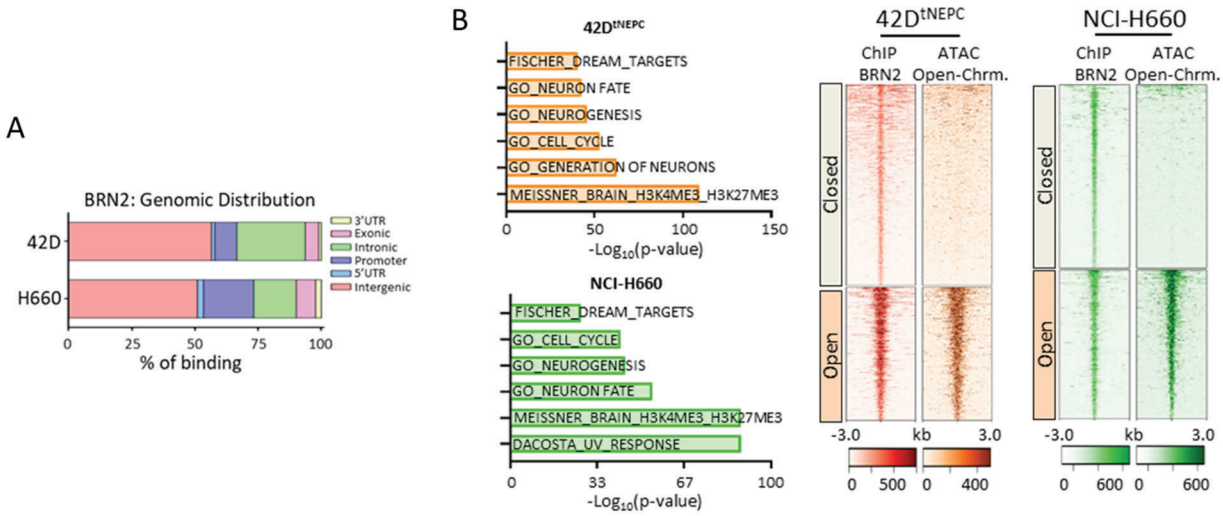

Figure 1 – A) Genomic distribution of BRN2 binding sites relative to gene bodies within the chromatin. **B-C)** Pathway analysis from genes mapped to BRN2 binding sites in the genome in tNEPC 42D^{ENZR} and de novo NEPC NCI-H660 model **D)** Heatmap overlay of BRN2 bound peaks with ATAC-seq peaks for open/closed regions of chromatin in NEPC models.

Figure 2 – Histone modification profiling of tNEPC accessible DNA profile

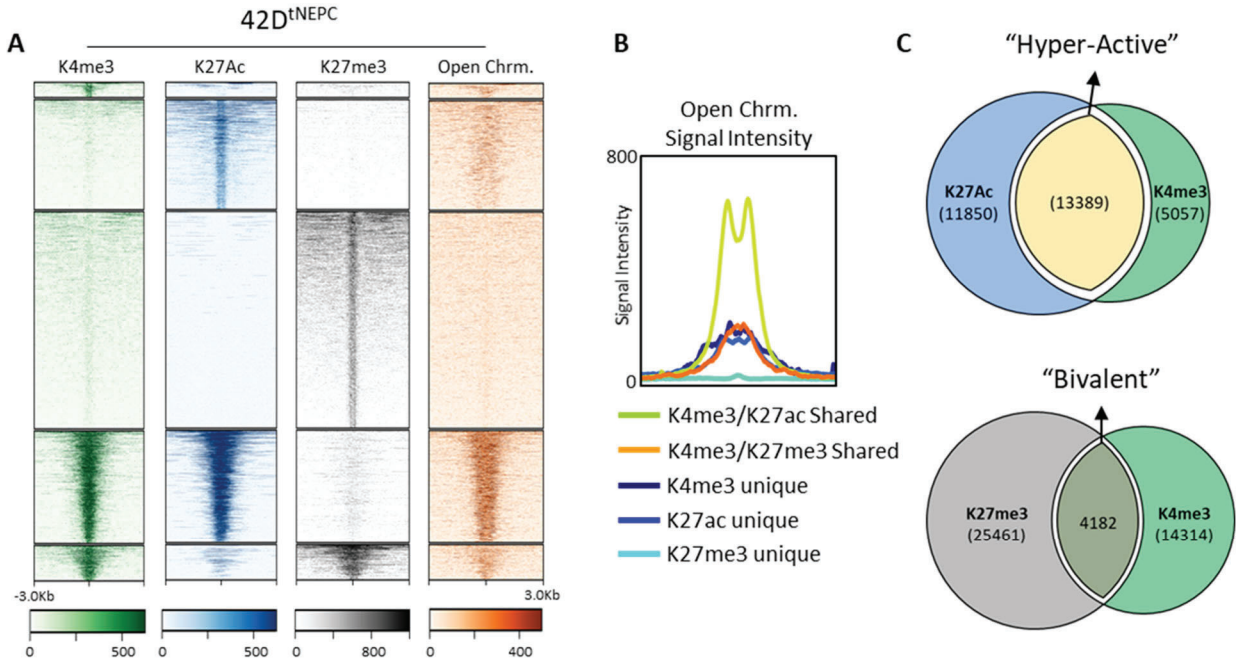

Figure 2 – A) Heatmap of H3K4me3, H3K27Ac and H3K27me3 occupied regions with ATAC-seq peaks for open/closed regions of chromatin in NEPC models. **B)** Average ATAC-seq signal intensity within different co-bound and unique regions for H3K4me3, H3K27Ac and H3K27me3. **C)** Venn diagram representation for overlapping regions between K4me3 and K27Ac dubbed "Hyper-Active" as well as overlap between K4me3 and K27me3 dubbed "Bivalent".

Figure 3 – BRN2 cistrome in tNEPC 42D^{ENZR} cells

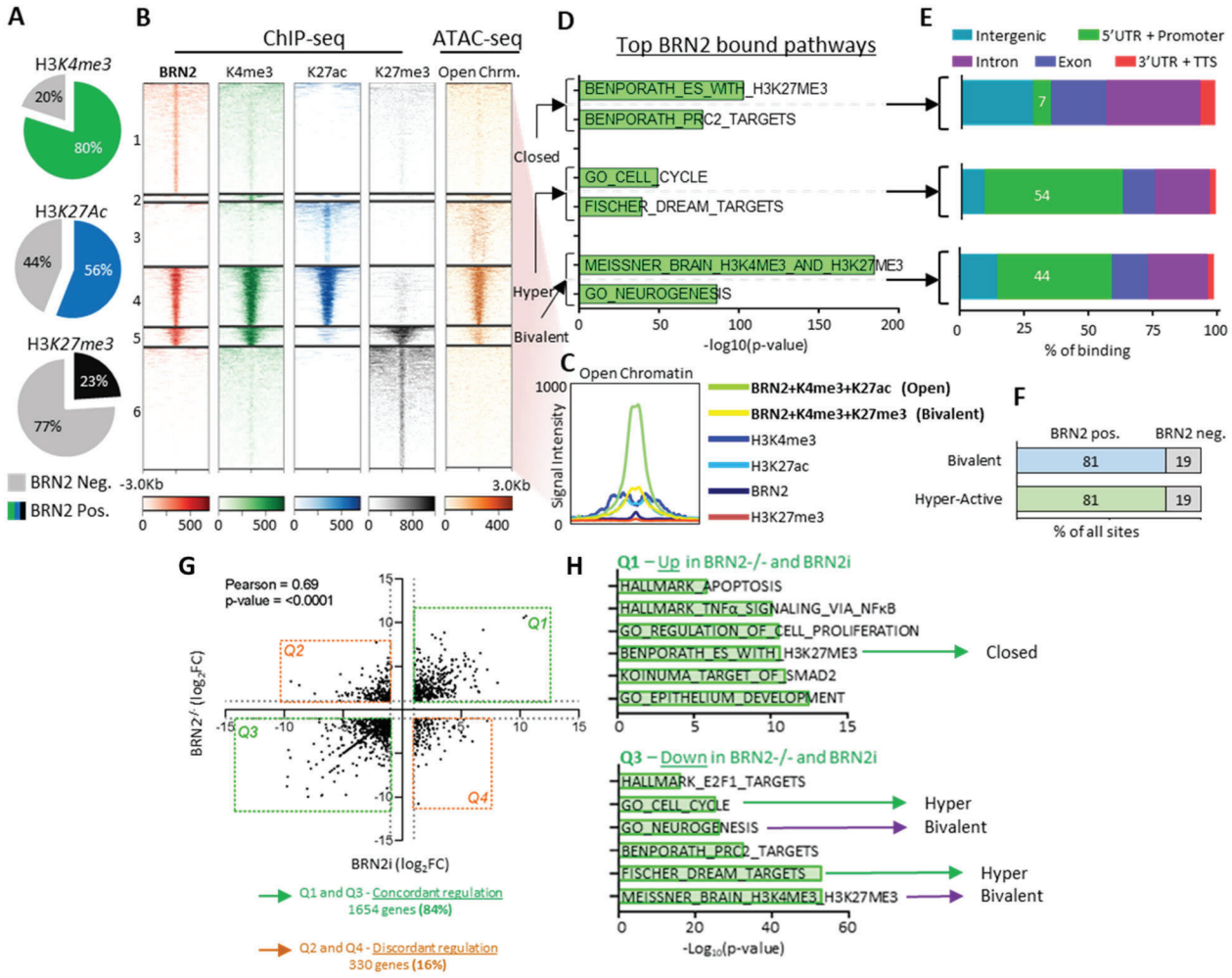

Figure 3 – A) Pie chart showing the percentage of each histone modifications co-occupied by BRN2 **B)** Heatmap of BRN2, H3K4me3, H3K27Ac and H3K27me3 unique and co-occupied regions with ATAC-seq peaks for open/closed regions of chromatin in NEPC models. **C)** Average ATAC-seq signal intensity within different co-bound and unique regions for H3K4me3, H3K27Ac and H3K27me3. **D)** Gene set enrichment genes mapped to BRN2 bound "Closed", "Hyper" and "Bivalent" regions. **E)** Genomic distribution of BRN2 binding sites relative to gene bodies within "Closed", "Hyper" and "Bivalent" regions. **F)** Percentage of "Hyper" and "Bivalent" regions positive for BRN2 binding. **G)** RNA-seq comparing log2(Fold Change) between BRN2-/- and BRN2i treated 42D^{ENZR} cells. **H)** Pathways enriched in each quadrant with concordant and discordant regulation of genes between BRN2-/- and BRN2i and cross-identification back to BRN2 cistrome regions.

Figure 4 – Efficacy of BRN2 inhibitor vs Carboplatin

A

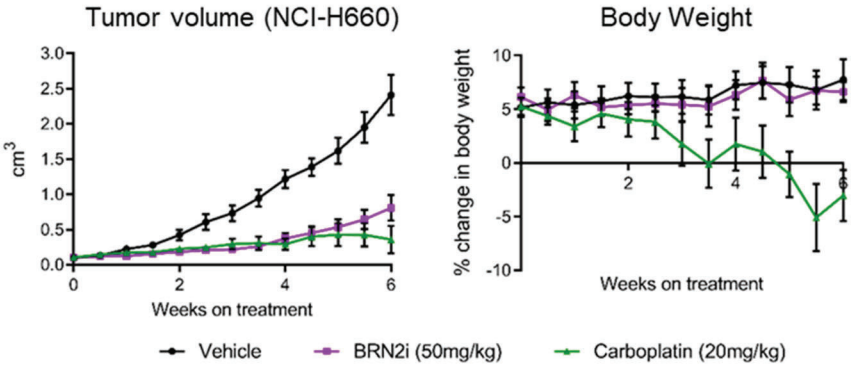

Figure 4 – **(A-B)** Xenograft of NCI-H660 injected into Nu/Nu mice. Mice were treated with indicated doses of BRN2i and Carboplatin when tumor volume reached 100mm^3. **A)** Tumor volume of 42D xenografts treated with control (n=5), 50mg/kg of BRN2i (n=5) and Carboplatin (n=5) **B)** Percent change in bodyweight of the mice since injection of tumor cells at the beginning of the study. Graph contains timepoints the mice were on treatment.

Figure 5 – BRN2 inhibition reduces production and secretion of IGFBP5

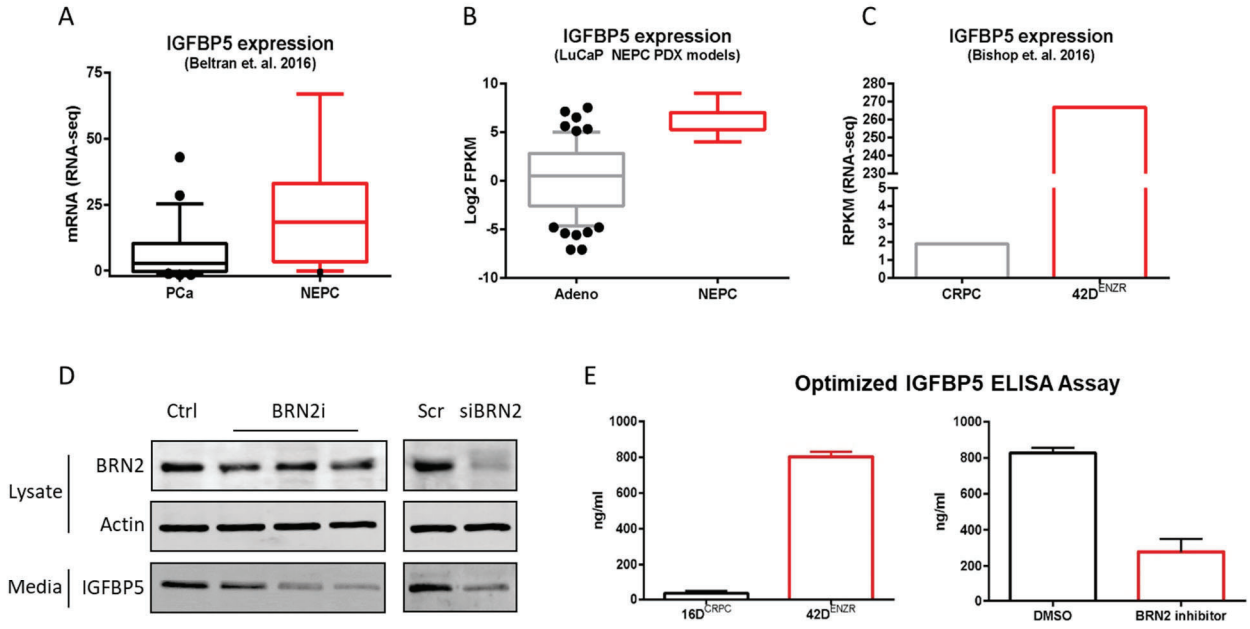

Figure 5 - A-C) mRNA expression of IGFBP5 in: **A)** NEPC patients from the Beltran et al. cohort (2016), **B)** Collection of LuCaP PDX models, **C)** $42D^{ENZR}$ versus $16D^{CRPC}$ using RNA-seq. **D)** Western Blot analysis of BRN2 and Actin from cell lyste and IGFBP5 from concentrated media of $42D^{ENZR}$ cells either treated with different BRN2i scaffolds treated at 5µM for 48 hours or with siRNA at 10nM for 48 hours. **E)** ELISA assay comparing secreted IGFBP5 in 16DCRPC cells and 42DENZR cells and in 42DENZR cells treated with BRN2 inhibitor at 5µM for 48 hours.

Figure 6 – Effect of AR inhibition of IGFBP5 expression and secretion

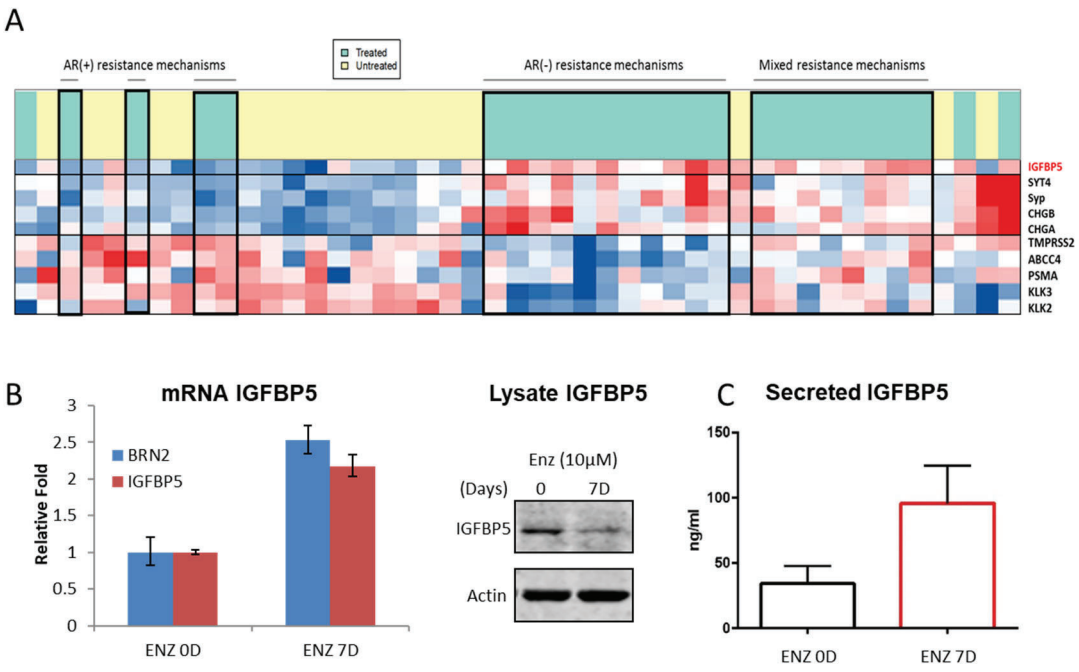

Figure 6 - A) Heatmap of mRNA from tumors NHT treated patients. Normalized gene expression from Nanostring **B)** 16D^{CRPC} cells treated with 10µM of ENZ for 7 days are subject to qPCR analysis for BRN2 and IGFBP5 and WB for IGFBP5. **C)** ELISA assay measuring secreted IGFBP5 from 16D^{CRPC} cells treated with 10µM of ENZ for 7 days.